

# Optical Frequency Comb Generated with an Amplitude Modulated Pump in Silicon Nitride Ring-resonators

Jose M. Chavez Boggio<sup>1</sup>, Daniel Bodenmüller<sup>1</sup>, S. A. Ahmed<sup>1,2</sup>, Adnan M. Baig<sup>1,2</sup>  
and Martin M. Roth<sup>1</sup>

<sup>1</sup>*innoFSPEC-VKS, Leibniz Institute für Astrophysik Potsdam (AIP), An der Sternwarte 16, D-14482 Potsdam, Germany*

<sup>2</sup>*Institut für Physik und Astronomie, Potsdam Universität, Potsdam, Germany*  
*jboggio@aip.de, dbodenmueller@aip.de*

Keywords: Optical Frequency Combs, Silicon Nitride Ring-resonator, Soliton.

Abstract: The coherence of the repetition-rate of optical frequency combs when generated using an amplitude modulated pump is experimentally investigated. We show that the repetition-rate of the frequency comb exhibit a linewidth of  $\sim 25$  Hz even when the mismatch between the modulation frequency and the resonator free-spectral range is larger than the linewidth of the resonances of the ring-resonator.

## 1 INTRODUCTION

State-of-the-art complementary metal-oxide semiconductor (CMOS) technology allows the precise fabrication of photonic circuits with nanometer-level accuracy, potentially enabling the merging of electronic and photonic components on a chip. CMOS-compatible materials have received increased attention in the last few years for nonlinear on-chip devices (Foster et al., 2006) (Jalali, 2007) (Leuthold et al., 2010) (Zajnulina et al., 2014) (Chavez Boggio et al., 2014a) (Chavez Boggio et al., 2016) (Cohen et al., 2018) (Xue et al., 2019). Optical frequency combs (OFCs) generated in high quality-factor ( $Q$ ) silicon nitride ( $\text{Si}_x\text{N}_y$ ) ring-resonators is an example of such a miniature device. By pumping the ring-resonator with a continuous-wave (CW) laser, it has been demonstrated the generation of frequency combs with octave spanning bandwidths (Okawachi et al., 2011) (Papp et al., 2013) (Wang et al., 2017) (Hendry et al., 2019). However, fully coherent OFCs require the formation of solitons which are obtained through a complex pump wavelength tuning with very precise scanning speed and range. Furthermore, small changes in the intra-cavity power lead to temperature changes and therefore to changes of the free-spectral range (FSR) of the resonator. In (Del'Haye et al., 2012), it was shown that 1 mW of power fluctuation can lead to a change of 6 kHz in the FSR. This impose that an active stabilization mechanism has to be implemented in order to generate OFCs with stable repetition-rates.

Recently, it has been proposed that by injecting a modulated pump in the ring resonator with a frequency matching its FSR, the threshold for frequency comb generation is much lower than by using a CW pump. Furthermore, the pump to frequency comb conversion efficiency is much higher than for the CW case (Obrzud et al., 2017). It was also shown that the stability of the modulation signal is transferred to the repetition-rate of the OFC, opening the possibility of ultra-stable devices. The OFC repetition-rate stability is a critical characteristic not only for spectroscopic or metrological applications but also for the calibration of astronomical spectrographs (Chavez Boggio et al., 2014b) (Zajnulina et al., 2015) (Chavez Boggio et al., 2018). It was experimentally shown that by varying the driving external modulation frequency, the soliton pulse repetition-rate could adiabatically follow the external frequency up to a frequency mismatch of 60 kHz and then the soliton (frequency comb) is annihilated (Obrzud et al., 2017). The authors calculate the change of the FSR of the resonator corresponding to the heating effect when the laser wavelength matches the resonance. This change is only a few kHz, which is much smaller than the reported mismatch tolerance. Even though this makes a tight compromise and reduce the practicality of such approach. In this paper we experimentally demonstrate that the external modulation can have a mismatch in excess of several hundred of MHz with respect to the FSR (larger than the linewidth of the resonances in our resonator) and still produce stable OFCs.

Section 2 describes our experimental arrangement

and procedure, while section 3 describes the experimental results. Finally in section 4 we draw our conclusions.

## 2 EXPERIMENTAL SETUP

A tunable laser centered at  $\lambda_p = 1568.7$  nm and providing 12 mW continuous wave (CW) power serves as the pump. The pump light is amplitude modulated using a LiNbO<sub>3</sub> modulator. A signal generator drives the modulator with a frequency nearly matching the spacing between the resonances in our ring-resonator. With a bias voltage, the shape of the modulation is adjusted to maximize the optical frequency comb bandwidth. The modulated light is splitted with a 1/99 splitter and its spectrum is monitored through the 1% port using an optical spectrum analyser (OSA). The 99% port is directed into an Erbium-doped fiber amplifier (EDFA) where the pump is amplified to a nominal power of 3.5 W. The amplified light is then propagated through a band-pass optical filter in order to filter out the amplified spontaneous emission noise from the EDFA. With a polarization controller, the polarization of the pump is adjusted in order to match the quasi-TE mode of the ring-resonator. The pump light is injected into the chip by either using a fiber lens or an objective lens (having NA 0.85). The silicon nitride ring-resonator has a radius of  $\sim 800 \mu\text{m}$  resulting in resonances spaced by 28.55 GHz.

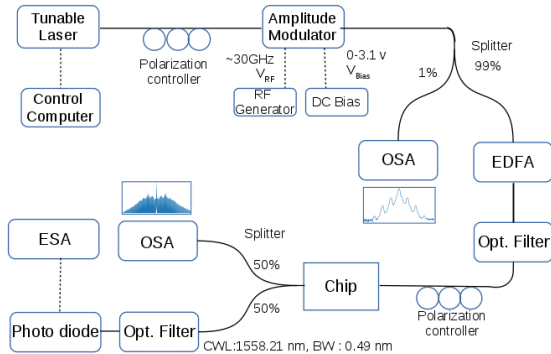


Figure 1: Experiment setup for frequency comb generation.

The measured  $Q$ -factor of the resonator is  $\sim 2 \times 10^6$ , corresponding to a resonance linewidth of  $\sim 100$  MHz. The ring-resonator transversal dimensions are: width =  $1.7 \mu\text{m}$  and height =  $800$  nm. The chip contains inverse tapered bus-waveguides to in- and out-coupling the light. The nominal losses are 2 dB for each end. The gap between the bus waveguide and the ring is 550 nm which corresponds nearly to critically coupling the light into the resonator. The

pump power coupled into the chip is estimated to be 400 mW. The generated frequency comb light is out-coupled from the chip using a lensed fiber and then splitted in 50/50. One part is directed to a band-pass optical filter (center  $\lambda = 1558.21$  nm and bandwidth = 0.49 nm). This allows to filter out two comb lines of the generated OFC. The beat note of the comb lines is detected with a high-speed photodiode and visualized with an electrical signal analyser (ESA). The other splitter arm is connected to an OSA (0.05 nm resolution bandwidth) for the visualization of the frequency comb spectrum.

## 3 EXPERIMENTAL RESULTS

The spectrum of the pump laser after the amplitude modulation is performed is shown in fig. 2. In the time domain this corresponds to a pulse train having a repetition-rate of 28.55 GHz. The more contiguous sidebands to the central pump are only 5 dB lower in power, indicating a strong modulation. The pulse width of this pulse train is estimated to be 25 ps. The dissipative Kerr solitons (DKS) formation in the ring-resonator is expected to be locked to the repetition-rate of this initial pulse train and the generated soliton will sit on top of the initial pulses.

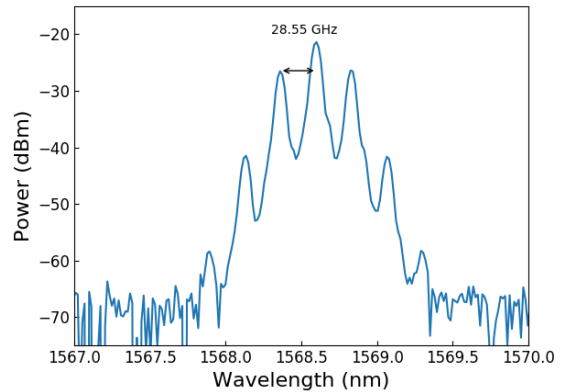


Figure 2: Spectrum of the amplitude modulated pump.

Fig. 3 shows the frequency comb spectrum when the amplitude modulation was set to 28.55 GHz, which corresponds to the resonator FSR. The OFC exhibits a  $\pm 15$  dB bandwidth of 100 nm. Over this bandwidth the OFC has 430 comb lines. It is estimated that the pump to comb lines conversion efficiency is 10%, which is much larger than when the OFC is generated using a CW pump. The inset shows a zoom of the generated frequency comb in the region 1550 - 1560 nm. The smooth spectral envelop shape approaches a  $\text{sech}^2$ -shape, which is typical of DKS.

Contrary to CW pumped resonators, where reliable generation of DKS is challenging, by using a modulated pump it is straight forward.

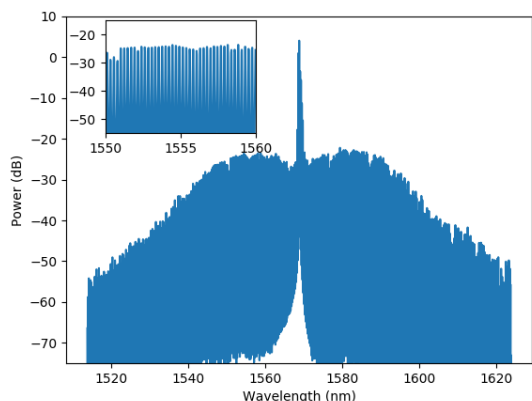


Figure 3: Frequency comb spectrum obtained when the amplitude modulation frequency is set at  $f = 28.55$  GHz.

By optically filtering two frequency comb lines around 1558 nm, we could measure their beat note using a fast photodiode and assess the noise characteristics of the repetition-rate of the OFC. The ESA resolution was set at 2 kHz. Fig. 4 shows the spectrum of the repetition-rate signal over a 100 MHz bandwidth and centered at the modulation frequency (28.55 GHz). There is negligible noise build-up for the spectral components different than the modulation frequency (28.55 GHz), indicating that the DKS perfectly acquires the external modulation frequency while other spectral components are completely negligible.

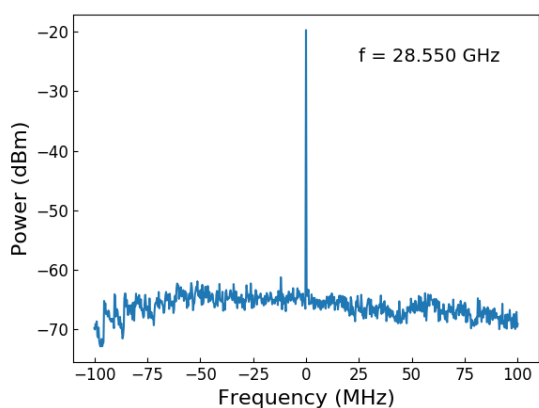


Figure 4: Beat note of the frequency comb repetition-rate.

Fig. 5 shows the frequency comb spectrum obtained when the modulation frequency was set at 28.68 GHz. This is 80 MHz larger than the FSR of the resonator and larger than the linewidth of the res-

onance (100 MHz). Note that the spectrum is less round than in Fig. 3, but has a bump of intensity at 1560 and 1580 nm. This is an indication that not only a fundamental soliton is being generated but a higher-order soliton (with low power) also propagates in the ring-resonator.

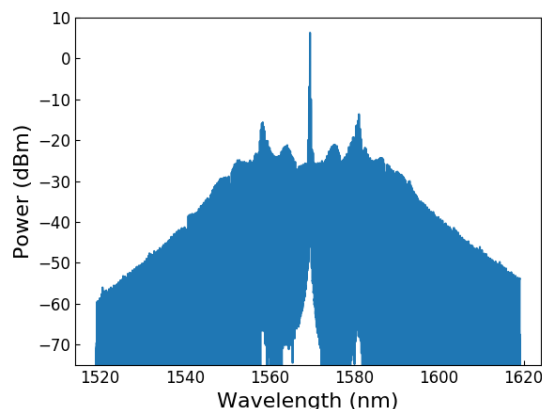


Figure 5: Frequency comb spectrum obtained when the amplitude modulation frequency is set at  $f = 28.68$  GHz.

The repetition-rate of the frequency comb obtained with a resolution bandwidth of the ESA set at 20 Hz is shown in fig. 6. The linewidth of the frequency comb repetition-rate is comparable to the resolution bandwidth of the electrical spectrum analyzer (20 Hz). In (Obrzud et al., 2017), it was reported that the mismatch between the modulation frequency and the repetition-rate of the resonator could not be more than 60 kHz before the frequency comb collapses. In our experiment, we could continuously tune the modulation frequency by tens of MHz and the frequency comb adapts adiabatically and does not collapse during the tuning process.

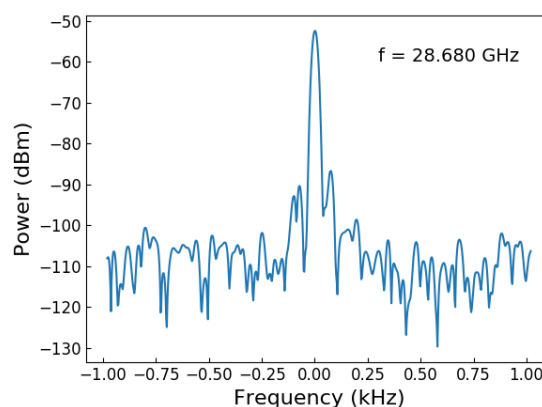


Figure 6: Repetition-rate of the frequency comb with a pump modulated at 28.68 GHz.

Fig. 7 shows the spectrum of the electrical signal driving the amplitude modulator taken with the ESA with a resolution bandwidth set at 20 Hz. This shows that as the frequency comb is generated it builds up from the exact external modulation frequency. The OFC repetition-rate linewidth exhibits negligible broadening if compared to the modulating signal, even though hundreds of comb lines are generated in a complex cascaded four-wave-mixing process (Sodre Jr et al., 2008).

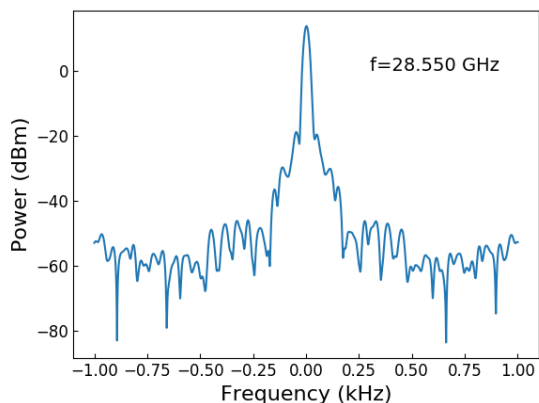


Figure 7: Spectrum of the electrical signal driving the amplitude modulator.

Fig. 8 shows the OFC generated when the modulation frequency is set to 28.77 GHz. Note that the spectrum is even more structured than the one in fig. 5. This indicates that as the modulation frequency shifts from the resonator FSR frequency, it is more difficult to generate a temporal fundamental soliton but there is also a high-order soliton co-propagating with the fundamental soliton.

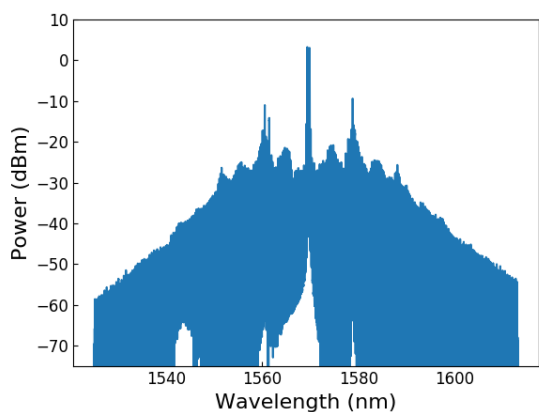


Figure 8: Frequency comb spectrum at  $f = 28.77$  GHz.

Fig. 9 shows the repetition-rate of the frequency comb. Even though it exhibits a narrow linewidth, sidebands grow considerably if compared to Fig. 7.

As the modulation frequency de-synchronizes further from the FSR of the resonator, the repetition-rate of the frequency comb becomes weaker in power and noisy and eventually a DKS can not be any longer generated. The largest de-synchronization for what we could still have a frequency comb repetition-rate, locked to the external modulation frequency, was  $\sim 600$  MHz. For that mismatch, the repetition-rate signal was very weak and noisy. For larger mismatches, the frequency comb could not operate locked at the external modulation frequency.

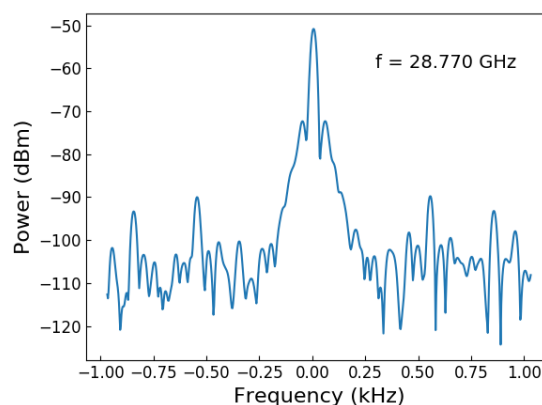


Figure 9: Repetition-rate of the frequency comb generated with a pump modulated at 28.77 GHz.

In (Obrzud et al., 2017) it was shown that the soliton central wavelength shifts as a consequence of the mismatch between the external modulating frequency and the FSR of the resonator. The experimental central wavelength shift was found to be 120 GHz for 30 kHz mismatch. With our parameters of 220 MHz shift, that would correspond to 840 THz. However from the spectra in Fig. 2, 5 and 8 no noticeable central wavelength shift can be observed.

## 4 CONCLUSIONS

Frequency comb generation using an amplitude modulated pump has been experimentally investigated. The modulation frequency was detuned from the free-spectral range of the resonator by several hundred of MHz in order to assess the robustness of the generated solitons under external modulation. Optical frequency combs with 100 nm bandwidth and repetition-rate of 28.55 GHz were generated. It was shown that the soliton is adiabatically locked to the external modulation frequency, even though the large mismatch with the FSR of the resonator. The linewidth of the repetition-rate of the OFC exhibit negligible broadening if compared with the linewidth of the modu-

lating signal. Our findings should open new avenues towards OFCs with ultra-stable repetition-rates.

## ACKNOWLEDGEMENTS

This work was supported by BMBF (Federal Ministry of Education and Research) through grants 03Z2AN11 and 03Z2AN12.

## REFERENCES

- Chavez Boggio, J., Bodenmüller, D., Fremberg, T., Haynes, R., Roth, M. M., Eisermann, R., Lisker, M., Zimmermann, L., and Böhm, M. (2014a). Dispersion engineered silicon nitride waveguides by geometrical and refractive-index optimization. *JOSA B*, 31(11):2846–2857.
- Chavez Boggio, J., Fremberg, T., Bodenmüller, D., Sandin, C., Zajnulina, M., Kelz, A., Giannone, D., Rutowska, M., Moralejo, B., Roth, M., et al. (2018). Wavelength calibration with pmas at 3.5 m calar alto telescope using a tunable astro-comb. *Optics Communications*, 415:186–193.
- Chavez Boggio, J., Fremberg, T., Moralejo, B., Rutowska, M., Hernandez, E., Zajnulina, M., Kelz, A., Bodenmüller, D., Sandin, C., Wyszomolek, M., et al. (2014b). Astronomical optical frequency comb generation and test in a fiber-fed muse spectrograph. In *Advances in Optical and Mechanical Technologies for Telescopes and Instrumentation*, volume 9151, page 915120. International Society for Optics and Photonics.
- Chavez Boggio, J., Moñux, A. O., Modotto, D., Fremberg, T., Bodenmüller, D., Giannone, D., Roth, M., Hansson, T., Wabnitz, S., Silvestre, E., et al. (2016). Dispersion-optimized multicladding silicon nitride waveguides for nonlinear frequency generation from ultraviolet to mid-infrared. *JOSA B*, 33(11):2402–2413.
- Cohen, R. A., Amrani, O., and Ruschin, S. (2018). Response shaping with a silicon ring resonator via double injection. *Nature Photonics*, 12(11):706.
- Del’Haye, P., Papp, S. B., and Diddams, S. A. (2012). Hybrid electro-optically modulated microcombs. *Physical Review Letters*, 109(26):263901.
- Foster, M. A., Turner, A. C., Sharping, J. E., Schmidt, B. S., Lipson, M., and Gaeta, A. L. (2006). Broad-band optical parametric gain on a silicon photonic chip. *Nature*, 441(7096):960.
- Hendry, I., Garbin, B., Murdoch, S. G., Coen, S., and Erkintalo, M. (2019). Impact of de-synchronization and drift on soliton-based kerr frequency combs in the presence of pulsed driving fields. *arXiv preprint arXiv:1905.09810*.
- Jalali, B. (2007). Teaching silicon new tricks. In *OFC/NFOEC 2007-2007 Conference on Optical Fiber Communication and the National Fiber Optic Engineers Conference*, pages 1–23. IEEE.
- Leuthold, J., Koos, C., and Freude, W. (2010). Nonlinear silicon photonics. *Nature photonics*, 4(8):535.
- Obrzud, E., Lecomte, S., and Herr, T. (2017). Temporal solitons in microresonators driven by optical pulses. *Nature Photonics*, 11(9):600.
- Okawachi, Y., Saha, K., Levy, J. S., Wen, Y. H., Lipson, M., and Gaeta, A. L. (2011). Octave-spanning frequency comb generation in a silicon nitride chip. *Optics letters*, 36(17):3398–3400.
- Papp, S. B., Del’Haye, P., and Diddams, S. A. (2013). Mechanical control of a microrod-resonator optical frequency comb. *Physical Review X*, 3(3):031003.
- Sodre Jr, A. C., Boggio, J. C., Rieznik, A., Hernandez-Figueroa, H., Fragnito, H., and Knight, J. (2008). Highly efficient generation of broadband cascaded four-wave mixing products. *Optics Express*, 16(4):2816–2828.
- Wang, Y., Leo, F., Fatome, J., Erkintalo, M., Murdoch, S. G., and Coen, S. (2017). Universal mechanism for the binding of temporal cavity solitons. *Optica*, 4(8):855–863.
- Xue, X., Zheng, X., and Zhou, B. (2019). Super-efficient temporal solitons in mutually coupled optical cavities. *Nature Photonics*, page 1.
- Zajnulina, M., Boggio, J. C., Böhm, M., Rieznik, A. A., Fremberg, T., Haynes, R., and Roth, M. M. (2015). Generation of optical frequency combs via four-wave mixing processes for low-and medium-resolution astronomy. *Applied Physics B*, 120(1):171–184.
- Zajnulina, M., Böhm, M., Blow, K., Boggio, J. M. C., Rieznik, A. A., Haynes, R., and Roth, M. M. (2014). Generation of optical frequency combs in fibres: an optical pulse analysis. In *Advances in Optical and Mechanical Technologies for Telescopes and Instrumentation*, volume 9151, page 91514V. International Society for Optics and Photonics.